DTU Library

Time domain PD-detection vs. dielectric spectroscopy

Holbøll, Joachim T.; Edin, Hans; Gäfvert, Uno

Published in:
IEEE 1997 Annual Report. Conference on Electrical Insulation and Dielectric Phenomena

Link to article, DOI:
10.1109/CEIDP.1997.641120

Publication date:
1997

Document Version
Publisher's PDF, also known as Version of record

Time Domain PD-detection vs. Dielectric Spectroscopy

J.T. Holbøll
Technical University of Denmark
Dept. of Electric Power Engineering
Building 325, DK-2800 Lyngby
DENMARK

U. Gäfvert
ABB Corporate Research
S-721 78 Västerås
SWEDEN

H.Edin
Royal Institute of Technology
Dept. of Electric Power Engineering
Teknikringen 33, S-100 44 Stockholm
SWEDEN

Introduction

The application of insulating diagnostic tools working in frequency domain on a time domain based phenomena like partial discharges (PD) leads to the question of the capabilities and limitations of such an approach.

Integrating detection systems have existed for many years, as, for example, the capacitance bridge method [1]. In order to establish a relationship between two newer techniques for insulation diagnostics, phase resolved partial discharge detection and dielectric spectroscopy, a common research project was started between the Technical University of Denmark and the Royal Institute of Technology in Sweden.

Some of the results have been presented earlier [2], mainly concentrating on the influence of test voltage and frequency on the results. In this paper, we will discuss the relationship on a theoretic and experimental basis.

Partial discharges measured by means of dielectric spectroscopy

In order to establish the relationship between partial discharges and the response from a diagnostic system that measures $\tan\delta$ at various frequencies, we consider a two electrodes system with a dielectric material in between. The dielectric includes a large number of internal voids, losses in the material itself are neglected, which means that the relative permittivity ε_r is real. On the two electrodes, we apply an AC-voltage $u(t)=u_0 \cdot \sin(\omega t)$ at frequency ω and a field strength high enough to generate partial discharges in the voids.

The discharges will induce charges on the electrodes, the free part of which is assumed to be compensated by a current i_{PD} from the detection system to the electrodes [3]. In this case, the discharges are assumed to be the only loss mechanism in the system and $\tan\delta$ is given by

$$\tan\delta = \frac{i_{PD,Loss}}{i_C}, \qquad (1)$$

where $i_{PD,Loss}$ is that part of the discharge current that contributes to the losses and i_C is the capacitive current through the system with a vacuum capacitance C_0:

$$i_C = \omega \cdot \varepsilon_r \cdot C_0 \cdot u_0 \qquad (2)$$

Due to the transient character of the discharges, we represent the current to the electrodes caused by each discharge, by a δ-function. This gives the total discharge current $i_{PD}(t)$:

$$i_{PD}(t) = \sum_i q_i \cdot \delta(t - t_i) \qquad (3)$$

where q_i is the total charge to the electrodes, caused by the i-th discharge, also called apparent charge.

Internal voids are known to give discharges at a phase position around or just after the zero crossing of the applied field [5]. The large number of voids combined with an electric field well above inception allows us to assume periodicity of the discharge pulses:

$$i_{PD,i}(t+T) = i_{PD,i}(t) \qquad (4)$$

where $T=2\pi/\omega$ is the period of the applied field and the discharge sequences. The PD-current , therefore, can be represented by a Fourier series:

$$i_{PD}(t) = \frac{a_0}{2} + \sum_{n=1}^{\infty} a_n \cos n\omega t + b_n \sin n\omega t\,, \qquad (5)$$

where a and b are the Fourier-coefficients:

$$a_n = \frac{\omega}{\pi} \int_0^{2\pi/\omega} i_{PD}(t) \cos(n\omega t) dt \qquad (6)$$

$$b_n = \frac{\omega}{\pi} \int_0^{2\pi/\omega} i_{PD}(t) \sin(n\omega t) dt \qquad (7)$$

Since the applied voltage is $u(t)=u_0 \cdot \sin(\omega t)$, it is obvious that b_1 is an expression for the lossy part of the discharge current and a_1 is an expression for the capacitive part.

(0-7803-3851-0) 1997 IEEE Annual Report - Conference on Electrical Insulation and Dielectric Phenomena, Minneapolis, October 19-22, 1997

In order to calculate the losses, (3) and (7) combined yield:

$$i_{PD,Loss} = \frac{\omega}{\pi} \cdot \sum_i q_i \sin(\omega t_i) \tag{8}$$

It can be seen that the discharge pulses contribute to the losses, depending on the time of their occurrence, i.e. their phase position. Inserting (2) and (8) in (1):

$$\tan\delta = \frac{\sum_i q_i \sin(\omega t_i)}{\pi \cdot \varepsilon_r \cdot C_0 \cdot u_0} \tag{9}$$

In a similar way, the discharges' influence on the measured capacitance can be determined. The change in capacitance can be calculated as $\Delta C = i_{PD,Cap}/\omega u_0$, where the capacitive part of the discharge current is given by combining (3) and (6):

$$i_{PD,Cap} = \frac{\omega}{\pi} \cdot \sum_i q_i \cos(\omega t_i) \tag{10}$$

In order to be able to calculate the expected loss factor, the temporal distribution of q_i has to be known. In the present investigations, it is given by the phase and height distributions of the discharge pulses. These distributions are influenced by a large number of parameters and aging effects. Nevertheless, certain defect types such as internal voids and corona, can result in PD-pulses at specific phase positions, the measurement of which are known as PD-patterns. The influence of the phase position on the measured loss angle can be illustrated in the following way:

Consider two types of partial discharges, corona and internal discharges, typical phase positions and polarities of the pulses are shown in fig.1. Their influence on the loss factor is in (9) given by the sum of all $q_i \cdot \sin(\omega t_i)$.

Corona:

Corona pulses occur at fundamental frequency minimum and, if the voltage is high enough, at maximum. As q_i changes polarity at zero crossing of *sin(ωt)*, the loss factor, therefore, is affected by corona discharges.

Internal Discharges:

Under the assumption of an asymmetric distribution around fundamental frequency zero crossing (which is usually the case), the loss factor at this frequency will increase at discharge inception. But it has to be mentioned that a perfectly symmetric distribution around zero crossing will not affect *tanδ*. On the other hand, as shown in (10), the capacitive current and the measured capacitance will change, due to discharges symmetrically distributed around test voltage zero.

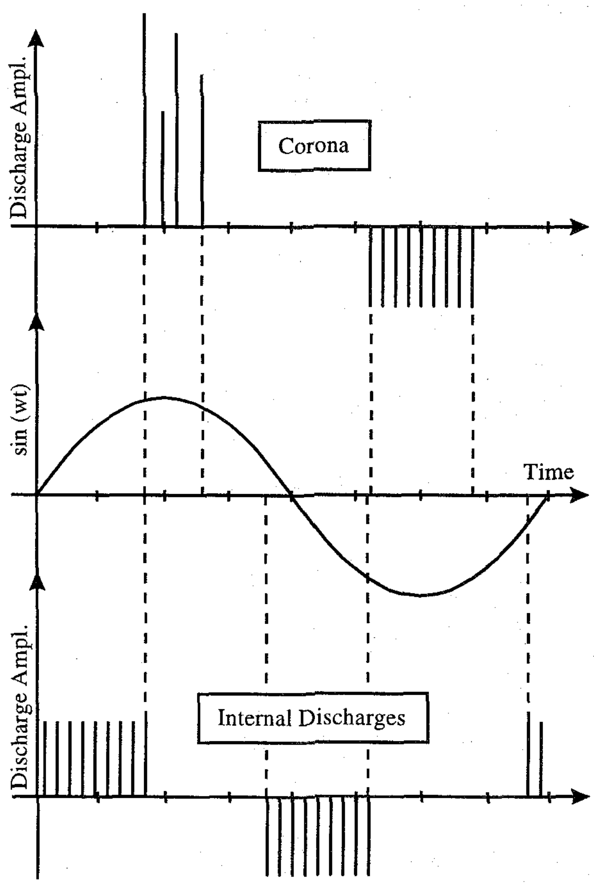

Fig. 1: Phase positions and polarities of discharge pulses related to applied voltage.

Experimental Set-up

In the following, the experimental work is described. Details of the set-up can be found in [2,4].

Test Object

An electric AC-field, with varying amplitude and frequency, is applied on 9 identical internal voids in epoxy. The voids were placed in such a way that a well defined charge displacement in each void would result in the same induced charge on the electrodes. The airfilled voids were 0.5mm high, 2mm in diameter and were placed at a distance of 2mm to each other in the middle of a disc of mica-filled, anhydride cured epoxy plastic, with 2.5mm thickness and a diameter of 100mm, as shown in fig.2.

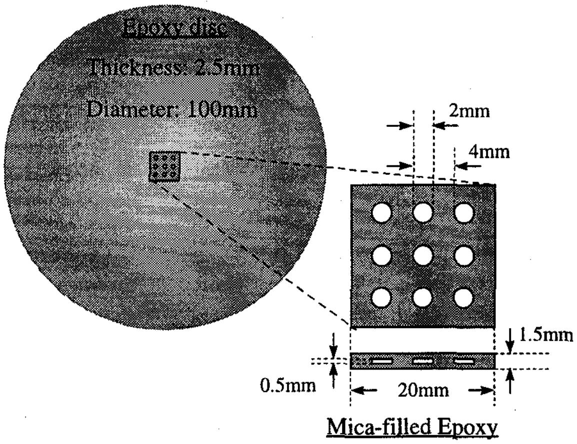

Fig. 2: Test sample with 9 cylindrical voids

Procedure

In order to minimize the influence of initial aging phenomena the sample was exposed to maximum voltage 20kV/50Hz for ½hour before the measurements. Hereafter, the measurements were run at stepwise decreasing voltage until PD-extinction. The loss measurements were repeated with increasing voltage until 20kV.

All voltages mentioned in the paper are peak voltages.

The measurements were done at 3 frequencies/decade in the 0.1 to 100Hz range (~0.1, 0.2, 0.5, 1.....100Hz). For the sake of clarity, some results presented in this paper are limited to the frequencies 0.1, 1, ~50Hz.

System for PD Measurements

Fig.3 shows the principle of the PD measuring system.

An 0-20kV$_{peak}$ AC voltage was applied to the electrodes in the test cell at varying frequencies between 0.1 and 100Hz. The test voltage was generated by a function generator and was amplified with a TREK 20/20A high voltage amplifier, the maximum current of which is limited to 20mA. High frequent noise from the amplifier made it necessary to include a low pass filter on the HV-side.

The apparent charge was measured as the peak value of the voltage pulse across an L-R measuring impedance, dimensioned to reduce the oscillations of the pulse to 6μs duration. The peak voltage of the amplified pulse was measured and analyzed by an ICM partial discharge analyzer (Power Diagnostix Systems), connected to a PC that controlled the measuring process and stored the data.

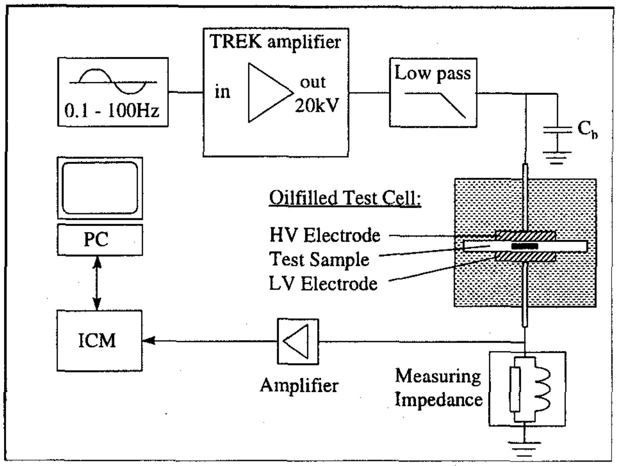

Fig. 3: System for PD-Detection

System for Dielectric Spectroscopy

Fig.4 shows the principle of the system for loss and capacitance measurements at variable frequencies.

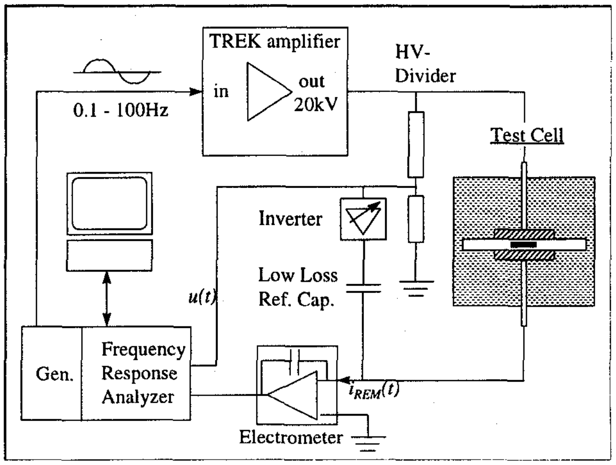

Fig. 4: Test system for dielectric spectroscopy

This system was built up around a frequency response analyzer, the voltage to which was taken from a HV-divider. Phase and amplitude of the current through the test sample were measured on the other channel of the analyzer. In order to increase the sensitivity of the system, the high capacitive current through the test sample was balanced by a current of opposite sign, generated by an inverter in series with a low loss reference capacitor of polypropylen. In balanced state, it was possible to resolve losses down to $1 \cdot 10^{-4}$ in tanδ.

Harmonic analysis could be done up to the 16th harmonic of the frequency of the applied voltage.

Noise and disturbances were suppressed by integration of the remaining current $i_{REM}(t)$ in an electrometer, together with a feedback capacitor.

The system was optimized to measure in the low frequency region, i.e. 0.1Hz-100Hz and less.

Results

Results from the PD-measurements are given as phase/height distributions, with the number of pulses given as a specific color in the diagram.

In fig.5 can be seen the PD-pattern at $17.8kV_{peak}$ test voltage run at 0.1Hz. The pattern shows more or less symmetry between positive and negative pulses and a phase position starting about 30 degrees before zero crossing, a pattern usually seen in the case of internal discharges [5].

The pulse height distribution changed slightly with frequency and test voltage and at lower voltages, the discharge inception point moved towards zero crossing. The symmetry between the two polarities was consistent.

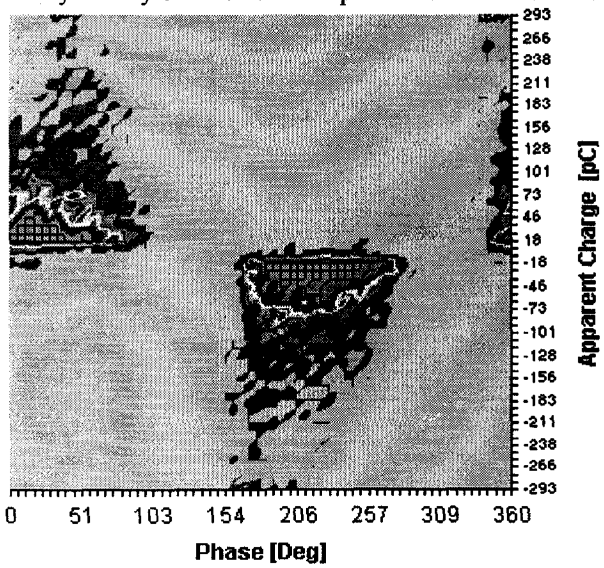

Fig. 5: Phase/height distributions of internal discharges at 17.8kV, 0.1Hz

A detailed description and discussion of this and other patterns is given in [2].

Since the pattern represents the distribution of PD-pulses $q_i(t)$, with respect to pulse amplitude and the phase of the applied voltage, it is, according to (9), possible to calculate $\tan\delta$ as a function of test voltage:

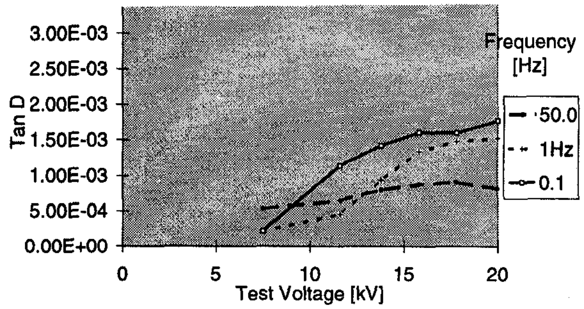

Fig. 6: Tanδ at 50, 1, 0.1 Hz based on results from PD-detection

As can be seen, the loss factor of $0.5\text{-}1\cdot10^{-3}$ is in the range of dielectric losses for epoxy without discharges. The increase rate is highest for low frequencies.

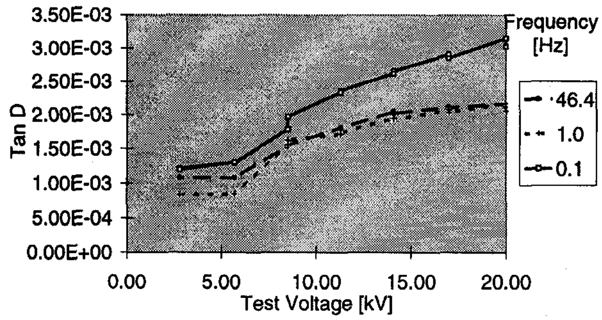

Fig. 7: Tanδ measured at 46, 1, 0.1 Hz by dielectric spectroscopy

Measurement of the loss factor as a function of test voltage with the system for dielectric spectroscopy (fig.7) gives values $\sim1\cdot10^{-3}$ higher, increasing with voltage and again with the highest losses at low frequencies. The offset deviation is obviously caused by non-PD losses in the material which are not included in (9). With this in mind, the agreement between the results from the two completely different methods is very good.

It has to be noted that the tanδ tip-up almost disappears at 0.1Hz, a fact that could make it difficult to identify the defect type at low frequencies.

For a thorough discussion of the results, we have to know the discharge activity as a function of applied voltage and frequency. This was done by calculating the total apparent charge per cycle and the results are shown in fig. 8.

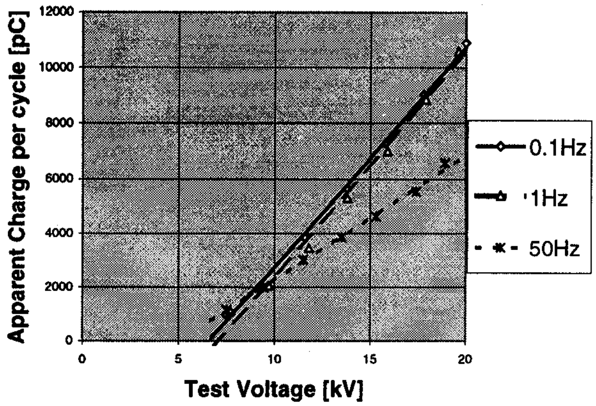

Fig. 8: Apparent charge per cycle measured as a function of applied voltage frequency

The apparent charge per cycle can be seen to increase linearly with test voltage amplitude, with the highest value at low frequencies.

Harmonic analyses of the current through the test object were done at all voltages and frequencies. Fig.9. shows the harmonics content related to the total current for 0.1Hz.

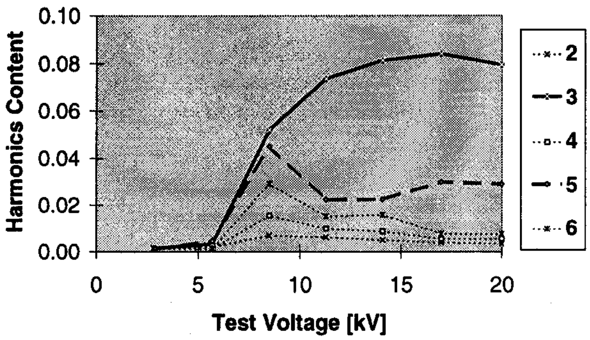

Fig.9: Content of harmonics (2^{nd}-6^{th}) in the current through the test object at 0.1 Hz.

It can be seen that the 3rd harmonic shows a very clear tip-up at PD-inception. The tip-up is also visible, but of less amplitude, at the other harmonics.

In fig.10 is shown an overview of the development of the harmonics as a function of test voltage amplitude and frequency. On the x-axis, the number of the harmonic is given for three frequencies and the y-axis is the test voltage amplitude.

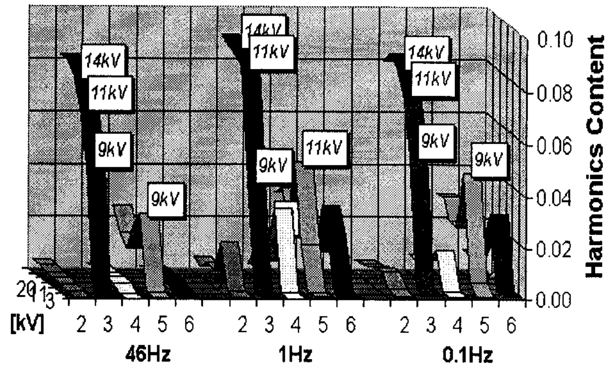

Fig.10: Content of harmonics (2^{nd}-6^{th}) in the current through the test object at 46, 1, 0.1 Hz.

It has to be mentioned that the shown harmonic content is in fact the content of the *integrated* current, since the system integrates i_{REM} in order to suppress the noise. In the correct expression, the content of harmonic number n in the current should be multiplied by n.

Discussion

The results confirm the well known fact that internal discharges, at least in this defect configuration, can be detected by dielectric loss measurements. The losses were shown to consist of dielectric losses and those caused by the internal discharges.

The calculated $tan\delta$, based on PD-detection, is in very good agreement with the loss measurements in frequency-domain, which confirms the validity of formula (9). This also means that the theoretically developed statement of defects, causing discharge pulse with symmetric phase distributions around test voltage zero, will not be detected by loss measurements.

The consequence of this is that $tan\delta$ measurements on high voltage equipment, always should be supplemented by measurements of capacitance.

The losses are highest at low frequencies, which is directly related to the dependency of the apparent charge/cycle on the applied voltage amplitude and frequency (fig.8). An identical dependency has also been measured (not shown here) with respect to the discharge activity per cycle and we will now discuss this behavior.

A large number of parameters have influence on the discharges, but there are two phenomena that are directly related to the temporal development of a discharge sequence: The release of an initiating electron and relaxation processes after the discharge.

Under the assumption of the statistical time lag for releasing an initiating electron being constant, very low frequencies will result in more discharges per cycle, since the influence of the time lag is reduced in the case of long cycles. This should be observable as a frequency dependent change of discharge inception with respect to phase position. This could not be observed. Relaxation processes after the discharges are, therefore, believed to be a more likely reason for the higher discharge activity at lower frequencies. Other physical aspects, including aging, are discussed in [2].

A major limitation to applications at low frequency test voltages is the disappearing of the tip-up at low frequencies. This means that the increasing losses at increasing test voltage can not necessarily be identified as partial discharges.

In order to overcome this problem, the very clear tip-up of the 3rd harmonic content in the current at discharge inception could be a solution. This tip-up is very clear at all test voltage frequencies and most of the odd harmonics. This phenomena has earlier been recognized for thermally aged stator bars at a test voltage frequency of 2Hz [6].

The explanation of this phenomena is obvious when considering fig.1: Since internal discharges mainly produce a PD-pattern symmetrical with respect to polarity, the odd components in the Fourier-series will dominate.

It was mentioned that the harmonic content in the current shown here is the harmonic content of the *integrated* current, thus emphasizing the lower harmonics. A mathematical correction of the result is possible, but it will cause a less signal-noise ratio. With respect to diagnostic systems, the reliability of the insulation condition assessment is the most important aspect, and a presentation such as the above is considered to be preferable.

In this paper, only loss measurements have been considered, i.e. the imaginary part of the complex permittivity. The real part, representing the capacitance, of course, is affected by the discharges as well and the possibilities of defect identification via the changes in both parts would be interesting for practical insulation diagnostics.

The work has to be followed up with investigations on other types of defects and other partial discharges, such as surface discharges and corona. Based on the above considerations on symmetry, other harmonic 'patterns' can be expected. Possibly, PD-patterns in the frequency-domain could be obtained, as known from time-domain analysis. Combined with the voltage/frequency dependency of $\underline{\varepsilon}$, quite a powerful diagnostic tool could be developed.

Conclusion

A theoretically developed relationship between partial discharges and the response from a system for dielectric spectroscopy was experimentally confirmed.

The losses caused by the discharges were highest at test voltages with low frequencies. At 0.1Hz, tanδ tip-up at discharge inception was very difficult to observe.

A very clear tip-up could be seen by detection of the third harmonic in the current through the test object. This is much more sensitive to the detection of internal partial discharges than traditional loss measurements, in particular when using low frequent test voltages.

References

[1] T.W. Dakin and P.J. Malinaric, "A Capacitance Bridge Method for Measuring Integrated Corona-Charge Transfer and Power Loss per Cycle", AIEE Trans. on Power App. and Sys., Vol. 79, No.3, Oct. 1960.

[2] J.T. Holbøll and H. Edin, "PD Measurements in Frequency and in Time Domain at variable power frequencies." International Symposium on High Voltage Engineering, Montreal, Canada, 1997.

[3] A. Pedersen, G.C. Crichton, I.W. McAllister, "Partial Discharge Detection: Theoretical and Practical Aspects". IEE Proc., Science, Meas. and Techn., Vol.142, No.1, January 1995.

[4] P. Thärning, P. Werelius, B. Holmgren and U. Gäfvert, "High Voltage Dielectric Response Analyzer for Cable Diagnostics", 1993 Annual Report - Conf. On Electrical Insulation and Dielectric Phenomena, pp.745 - 750, 1993.

[5] B. Fruth and L. Niemeyer, "The Importance of Statistical Characteristics of Partial Discharge Data", IEEE Trans. of Electrical Insulation, Vol.27, pp.60 - 69, 1992.

[6] M. Lundmark and D. Ribbing, "Studies of loss tangent and harmonic content with low frequency HV dielectric response measurements in order to evaluate degradation in machine insulation", ABB Corporate Research Report SECRC/KJD/TR-93/018, 1993.